Published in Journal of Cleaner Production with doi: 10.1016/j.jclepro.2022.132869

Uncertainty-aware Energy Management Strategies for PV-assisted Refuelling Stations with Onsite Hydrogen Generation

Marcos Tostado-Véliz[1], Ali Asghar Ghadimi[2], Mohammad Reza Miveh[3], Mohammad Bayat[2], Francisco Jurado[1,*]

1 Department of Electrical Engineering, University of Jaén, 23700 EPS Linares, Jaén, Spain (e-mail: mtostado@ujaen.es (M.T.-V.), fjurado@ujaen.es (F.J.)).
2 Department of Electrical Engineering, Faculty of Engineering, Arak University, Arak 38156-8-8349, Iran (e-mail: a-ghadimi@araku.ac.ir).
3 Department of Electrical Engineering, Tafresh University, Tafresh 39518-79611, Iran (e-mail: miveh@tafreshu.ac.ir).
* Correspondence: fjurado@ujaen.es

Abstract. One of the main barriers for the wide penetration of fuel cell electric vehicles is the lack of proper infrastructures for hydrogen transportation that hinders the implantation of refuelling stations. This barrier could be overcome by deploying onsite hydrogen generators based on mature electrolysis and hydrogen storage technologies. This way, the necessity of hydrogen transportation is avoided. In addition, electrolysers can be onsite supplied by means of renewable generators like photovoltaic panels, while the produced hydrogen can also be destined to generate electricity through fuel cells thus obtaining a monetary revenue. Thereby, the economy of the system may be improved in order to make viable this kind of infrastructures. However, the optimal coordination of the different assets is challenging and requires the use of energy management tools to pursue the optimal performance of the installation. In this kind of infrastructures, the energy management problem is performed under substantial uncertainties; moreover, these unknown parameters have a very different character. Thus, while energy pricing and renewable generation can be forecasted using conventional techniques, refuelling demand is highly unpredictable. To this end, this paper proposes a novel stochastic-interval model for the optimal scheduling of photovoltaic-assisted refuelling stations. The new proposal uses interval notation to model the inherent uncertainty of renewable generation and energy pricing, while the vehicle demand is modelled using a more suitable approach based on scenarios. In this regard, a comprehensive stochastic model for fuel cell electric vehicles is developed, which is based on reported driving behaviour and common characteristics of commercial vehicles. To solve the problem subjected to uncertainties, an iterative solution methodology is developed which allows adopting risk-seeker and risk-averse operational strategies. A case study is analysed to validate the new proposal and discussing the importance of the different economic activities that can be exploited in refuelling stations. Results reveal the importance of selling energy to the grid in order to complement the revenues obtained from refuelling; however, this process is highly impacted by uncertainties and the operational strategy, observing variations up to 50 % in the total profit depending on the strategy adopted.

Keywords. Fuel cell electric vehicles; Photovoltaic; Uncertainty; Robust optimization.

Nomenclature

Indexes (Sets)	
$s(\mathbb{S})$	Scenario
v	Vehicle in the fleet
m	Possible arrival times for a vehicle in the fleet
$r(\mathbb{R})$	Representative scenario
$t(\mathbb{T})$	Time
$\boldsymbol{\Psi}$	Uncertainties modelled as interval numbers
$\boldsymbol{\Omega}_r$	Cluster of the r^{th} representative scenario
Superscripts & notations	
$Grid, buy/sell$	Utility grid (buying/selling processes)
PV	Photovoltaic
$FCEV$	Fuel cell electric vehicle
EZ	Electrolyser
FC	Fuel cell
HSS	Hydrogen storage system
$Comp$	Hydrogen compressors
det	Deterministic
opt/pes	Optimistic/pessimistic
$\underline{(*)}/\overline{(*)}$	Minimum/maximum value
$\widehat{(*)}$	Uncertain parameter
$[*]$	Interval number
Functions	
$E[*]$	Expected value of an interval number
$\mathrm{round}(*)$	It rounds to the nearest integer
$\mathrm{rand}(*)$	It yields a random number according to a distribution
$\mathrm{size}(*)$	It yields the elements in a set or cluster
Probability distributions	
$\Gamma(\varsigma)$	Gamma distribution with shape parameter ς
$\mathfrak{W}(y)$	Probability of driving y miles
$\mathfrak{D}(t)$	Vehicle trip distribution at t time instant
$\mathfrak{N}(\mu, \sigma)$	Normal distribution with mean μ and standard deviation σ
$\mathfrak{G}(t)$	Probability of refuelling at t time instant
Parameters & constants	
$\Delta\tau$	Time step (h)
$RD/\ RU$	Ramp down/up rate (kW)
η	Efficiency (p.u.)
LHV	Hydrogen lower heating value (kWh/kg)
γ	Conversion factor (p.u.)
$\mathcal{R}$	Gas constant (J/mol·K)
θ	Temperature (K)
v	Gas volume (m^3)
ζ	Mass molar of hydrogen (kg/mol)

ϱ	Dissipation factor (%)
ς^{Comp}	Energy consumption of compressors (kWh/kg)
ω	Probability (p.u.)
π	Hydrogen price ($/kg)
λ	Energy price ($/kWh)
χ	Operation and maintenance costs ($/kWh)
κ	Capital cost ($/kW)
T	Estimated lifecycle (h)
ϑ	Start-up and shutdown costs ($)
ξ	Uncertain level (p.u.)
NV	Expected number of refuelling events
RF	Expected amount of hydrogen refuelled (kg)
Decision variables	
p	Power (kW)
u	Commitment status (binary)
g	Hydrogen flow (kg)
on/off	On/Off status (binary)
SOP	State-of-pressure (bar)

1 - Introduction

1.1 - Context & motivation

The damaging effects of climate-changing are major concerns for nowadays society. In this regard, governmental entities aspire to reduce the dependency on fossil fuels [1]. One of the main measures consists on decarbonizing the mobility sector [2]. Since the early 2000's, ambitious programs have been launched in order to progressively reduce the fleet of conventional vehicles to replace them with low-emissions ones [3]. In this context, electric vehicles (EVs) have progressively gaining importance on the mobility industry, steadily incrementing their market penetration throughout the last decade [4]. Among the different technologies of EVs, fuel cell EVs (FCEVs) emerged in 2014 as an attractive alternative to conventional battery vehicles since, due to the high energy density of hydrogen storage systems (HSSs) [5], the electric autonomy of FCEVs resembles conventional vehicles [6]. First generation FCEVs used a 350-bar pressurized storage, while the current 2nd generation increased to 700-bar, which boosted up the autonomy of these vehicles that may achieve up to 500 miles of electric autonomy [7].

With the characteristics mentioned above, FCEVs overcome the limited autonomy of battery vehicles without difficulty, thus supposing an invaluable asset for decarbonizing of the transportation sector. Nevertheless, FCEV industry is still reduced in comparison with other technologies. According to [8], the FCEV registrations remain three orders of magnitudes lower than battery-vehicles. However, this trend may change in the following 20-30 years, especially if incentives to green hydrogen production continue growing [9]. Currently, one of the main barriers for FCEVs is the overall lack of refuelling stations worldwide. This is due to, unlike electric networks, hydrogen transportation systems are not widely deployed [10]. In this regard, refuelling stations with onsite hydrogen generation may be an attractive alternative. Such kind of infrastructures does not require

the implantation or extension of transportation systems since hydrogen can be produced through onsite electrolysers [11]. Moreover, the electrolysis process can be supplied from clean generators like photovoltaic (PV) panels, and mature hydrogen storage technologies might be exploited in order to properly manage eventual surplus renewable energy, thus improving the economy of the system [5]. Nonetheless, this process requires the coordination of different assets, which usually work under intense uncertain environments caused by unpredictable renewable generation, electricity price, or hydrogen demand. Thereby, as in the case of electric charging stations [12], the development and study of appropriate energy management tools become crucial for the wide implantation of PV-assisted refuelling stations (PVaRFSs).

1.2 - Energy management in PVaRFSs: literature review

In [13], a Mixed-Integer nonlinear programming (MINLP) model is developed for refuelling stations integrated with wind turbines for optimal participation in electricity markets. A stochastic-based approach for optimal planning of refuelling stations encompassing a power-to-gas chain was proposed in [14]. This model is Mixed-Integer linear programming (MILP) and is focused on a specific area of Ontario (Canada). The design tool is based on different Gaussian models for FCEVs demand and contemplate variations throughout the project lifetime. On the other hand, the ref. [15] studied various hybrid systems for supplying refuelling stations, performing an optimal planning analysis using the software Homer® [16]. This study concluded that the system formed by wind and PV units further reduces the levelized cost of hydrogen compared to standalone wind generators. Likewise, Homer® was used in [17] for a case study in Ismir-Cesme (Turkey), concluding that the levelized cost of hydrogen may vary from 7.526 to 7.866 $/kg depending on the configuration of the hybrid supply system.

Wilke et al. [18] studied a multi-carrier electric-heat district with integrated refuelling stations. This study performs for planning purposes over large time horizons, carrying out a techno-economic analysis for different layouts, thus concluding that PV sizing and energy tariff strongly affect the final optimal layout. The ref. [19] focuses on small vehicles, particularly bicycles. In this regard, this study analyses the viability of a PVsRFS for hydrogen bicycles in Croatia, for which real data was obtained from benchmark experiments. The study concluded that the considered refuelling layout counting with batteries and a metal-hydride HSS is techno-economically viable, being able to supply up to 5 bicycles per day. In [20], a MILP operational model for microgrids was designed. In this formulation, FCEV refuelling is considered through the electrolyser-storage-fuel cell (FC) chain. The influence and interaction of external agents are also modelled and analysed, whereas mathematical tricks are used to keep the model linear and tractable. A comprehensive energy management tool for multi-energy microgrids is developed in [21]. The proposed formulation is MILP and accounts for electric, hydrogen, and gas sub-systems. Charging stations for different vehicles are considered. In particular, FCEVs are refuelled through a medium-scale power-to-gas system, which is also devoted to refuelling natural gas vehicles.

A MINLP model for the optimal design of refuelling stations was proposed in [22]. This reference focused on the participation of these infrastructures in ancillary service markets. Various numerical results are presented concluding that revenues for the operator may increase by 16% if the different components are properly sized and designed. A hybrid stochastic-robust approach for multi-energy hubs was developed in [23]. This MILP model incorporates an HSS integrated with demand-response programs in both electric and thermal loads. In [24], the techno-economic viability of wind-powered refuelling stations at seven locations in South Africa was addressed. The study was

performed using Homer® and concluded that the cost of hydrogen ranges from 6.34 to 8.97 $/kg depending on the location of the station. Mansour-Satloo et al. [25] developed a robust approach for optimal operation of multi-energy microgrids with refuelling stations. The mathematical model uses Information Gap decision theory (IGDT) to handle uncertainties in renewable generation, while fuzzy decision-making is considered for multi-objective optimization.

The ref. [26] proposes a multi-objective scheduling model for multi-carrier energy hubs with integrated demand response initiatives. The considered layout includes a hydrogen-chain in which electricity and hydrogen can be generated to satisfy local demands and complement the role of renewable generators. This way, the damaging effects of conventional pollutant generators can be lessened. Likewise, uncertainty is also handled in [27] regarding the optimal integration of refuelling stations in active distribution networks. To this end, various stochastic profiles are combined with deterministic data referred to prices and equipment specifications, resulting in a MILP formulation that is tractable by average solvers and machines. In [28], an uncertainty-aware scheduling model for multi-energy microgrids was developed. This approach accounts for uncertainties in renewable generation, energy price, and FCEV demand, for which different uncertainties models are considered.

1.3 - Gaps & contributions

This work is motivated by various gaps encountered in other related works. For the sake of simplicity, Table 1 shows a summary of the related literature, and the main gaps detected are summarized below:

- Some references use complicate or non-practical nonlinear optimization models. Others use metaheuristic solvers or software-based routines. These formulations are non-modular and frequently entail unaffordable computational burdens [29].

- Uncertainties in the renewable generation are frequently neglected or modelled using simple stochastic-based approaches. This principle requires a priori knowledge about the distribution of the uncertain parameter and results in costly computational tools.
- FCEV refuelling demand presents a high unpredictable behaviour which is challenging to handle. This aspect is usually ignored in the literature or simple stochastic models are used, which lack of sufficient accuracy and comprehensiveness [14, 27, 28].
- Most of the studied references deal with incomplete hydrogen chains that lack of the returning path through FCs. This way, the possibility of selling back energy to the grid is not contemplated, and possible revenues from this process cannot be evaluated. In addition, the majority of the analysed references are focused on planning horizons, while operational tools have been few studied so far.

Table 1. A summary of the related literature

Reference	Model	Uncertainties	FCEVs	FC	Horizon
[13]	MINLP	No	Deterministic	No	Operation
[14]	MILP	--	Stochastic	No	Planning
[15, 17, 24]	Homer	--	Deterministic	No	Planning
[18]	Metaheuristic	--	Deterministic	Yes	Planning
[18]	Experimental	--	Deterministic	No	Planning
[20]	MILP	No	Deterministic	Yes	Operation
[21]	MILP	No	Deterministic	No	Operation
[22]	MINLP	--	Deterministic	No	Planning
[23]	Robust MILP	Stochastic	--	Yes	Operation
[25]	MILP	IGDT	Deterministic	Yes	Operation
[26]	MILP	Stochastic	--	Yes	Operation
[27]	MILP	Stochastic	Stochastic	No	Planning
[28]	MILP	IGDT-Stochastic	Stochastic	Yes	Operation
Present	MILP+QP	Interval	Stochastic	Yes	Operation

To overcome the limitations above, this paper develops a novel scheduling tool for PVaRFSs. The developed methodology aims to account for a variety of uncertainties that arise from renewable generation, energy pricing and FCEV demand. These uncertainties,

however, have very different characteristics. Thus, while PV generation and energy price can be easily forecasted, FCEV demand presents a highly random behaviour. These particularities make unsuitable to use the same model for the different unknowns. To take into account the different character of uncertainties, a novel stochastic-interval approach is presented, by which PV generation and energy prices are modelled using interval notation, while highly unpredictable FCEV demand is handled via scenarios. This way, different uncertainties approaches are used, for convenience in the character of the uncertain parameter. As seen in Table 1, the present work supposes the first attempt to apply such approaches in PVaRFSs. Other salient contributions of this research are mentioned below:

- The developed model combines MILP and quadratic-programming (QP) formulations, being so modular and efficiently solvable by standard solvers [30].
- To overcome the lack of proper stochastic models for vehicles' demand, this paper develops a comprehensive scenario generator for FCEV demand, which is based on the well-reported driving behaviour of vehicles and commercial FCEV models. This way, the unpredictable behaviour of vehicles can be caught and integrated into the operational tool.
- Unlike refuelling demand, PV generation and energy price can be easily forecasted using conventional tools [31]. In this regard, stochastic programming may be unsuitable because the lack of historical data or probability functions. Thus, an interval-based approach is proposed to model these uncertainties, which can easily accommodate the stochastic-based approach used for vehicles' demand.
- The considered system enables the possibility of selling energy to the grid through FCs to obtain a revenue. This comprehensive modelling allows to further analyse refuelling installations. To this end, a novel iterative solution procedure is

developed, which permits to assume risk-seeker and risk-averse strategies. Making use of this methodology, a profuse analysis of refuelling infrastructures is addressed through simulations.

In the rest of this paper, Section 2 presents the necessary background. Section 3 describes the mathematical models. Section 4 presents the developed stochastic model for FCEV demand. Section 5 develops a solution methodology based on interval formulation and risk-seeker/risk-averse operational strategies. Section 6 presents a case study with results. This paper is concluded with Section 7.

2 - Preliminaries

2.1 - Hydrogen chain description

In the PVaRFS under study, hydrogen is onsite generated through water electrolysis. To this end, mature technologies can be considered such as polymer electrolyte membrane (PEM), alkaline or solid oxide, among others [32]. After that, the gaseous hydrogen is stored in vessels to be posteriorly used for FCEV refuelling or electricity production through FCs. For the sake of self-sufficiency, Table 2 describes the reaction that occurred in a PEM electrolyser/FC system [33]. In essence, water and oxygen react with electricity in the electrolyser to generate hydrogen, while the hydrogen molecules are decomposed in the FC to trigger electricity flow between the anode and the cathode.

Table 2. Overall reactions in water electrolysis and FC

	Electrolyser	**FC**
Anode	$2OH^- \rightarrow H_2O + 0.5O_2 + 2e^-$	$H_2 \rightarrow 2H^+ + 2e^-$
Cathode	$2H_2O + 2e^- \rightarrow 2OH^- + H_2$	$0.5O_2 + 2H^+ + 2e^- \rightarrow H_2O$

The gas flow generated in the electrolyser can be modelled as [34]

$$g_t^{EZ} = \frac{Q^{EZ}(\theta^{EZ}, J^{EZ})}{2 \cdot f \cdot V_t^{EZ}} \quad (1)$$

where Q^{EZ} is a nonlinear function of the temperature and current density J, f is the Faraday constant, and V^{EZ} represents the voltage drop across the electrolyser cell stack.

The dynamics on the hydrogen tank can be represented as a function of the instantaneous inflow/outflow gas rates ($g_t^{HSS,in}$ / $g_t^{HSS,out}$), as follows

$$\frac{v^{HSS}}{\mathcal{R}\cdot\theta^{HSS}}\cdot\frac{d}{dt}\cdot SOP_t^{HSS} = g_t^{HSS,in} - g_t^{HSS,out} \quad (2)$$

In energy management applications, fast dynamic effects are neglected as the time step $\Delta\tau$ is normally large enough to achieve the steady-state conditions between consecutive time slots [35]. Thus, under steady-state conditions, the inflow/outflow gas rates in (2) equal the gas demand of the other devices, as said the equations (3) and (4).

$$g_t^{HSS,in} = g_t^{EZ} \quad (3)$$

$$g_t^{HSS,out} = g_t^{FC} - g_t^{FCEV} \quad (4)$$

2.2 - System description

This paper is focused on PVaRFSs with onsite hydrogen generation. A schematic diagram of the installation under study is shown in Fig. 1. The station is composed by a PV array and a hydrogen chain formed by electrolysers, storage stages, and FCs. Thereby, the power-to-hydrogen and hydrogen-to-power paths are both enabled [5]. The hydrogen chain is also devoted to FCEV refuelling. In this paper, the vehicle fleet is assumed to be formed mostly by second-generation FCEVs with 700 bar onboard storage [36]. In this sense, a compression stage is necessary just before the refuelling point. This compressor must be supplied from the electricity subsystem and may consume large amounts of energy [37]. The installation is connected to an upscale grid from which can purchase or sell energy in order to obtain a monetary revenue. All the involved assets are coordinated in a centralized fashion by the system operator. This agent receives forecast information regarding renewable generation and energy price to, on the basis of this information, perform the day-ahead optimal scheduling program of the installation with the aim of maximizing his own profit. Subsequent sections are devoted on mathematically addressing this problem subjected to strong uncertainties.

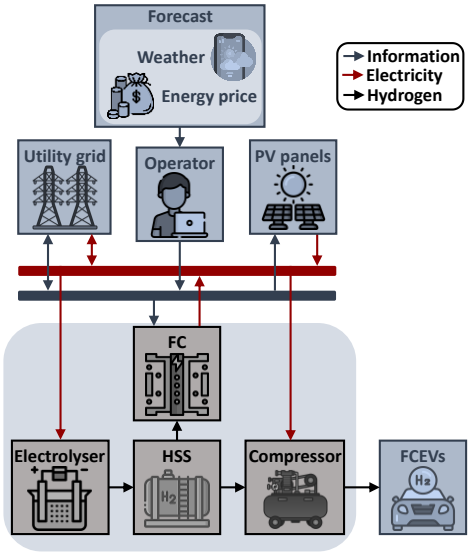

Fig. 1. Schematic diagram of the PVaRFS under study

3 - Mathematical modelling

This section presents the mathematical modelling of the components involved in the system described in Section 2. Such models are incorporated into the optimal scheduling problem as constraints. Moreover, a brief description of the interval notation used in this paper is provided, being referred to [5] for further information.

3.1 - Interval numbers

Interval numbers have been widely used to model uncertainties [38]. This approach is very suitable for representing unknowns that may lie with high probability within a predicted interval (confidence interval). Different interval notations have been used in the literature (e.g. see [39]); however, that developed in [5] has been used in this paper for its simplicity, whose foundation is sketched in Fig. 2. According to this formulation, an arbitrary interval number a can be mathematically expressed as follows

$$[a] \in \left[\underline{a}, \overline{a}\right] \tag{5}$$

$$[a] = \langle a | \underline{a} \leq E(a) \leq \overline{a} \rangle \tag{6}$$

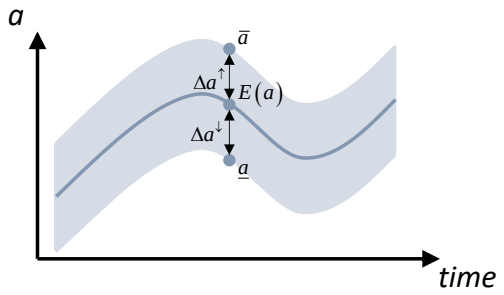

Fig. 2. Sketch of the interval notation used in this paper

Therefore, given the formulation above, the interval number a is fully defined by its expected (forecasted) value and its upper and lower bounds, which define the interval within which the unknown value may lie with high probability. Alternatively, the predicted interval can be written as

$$\Delta a^{\uparrow} = \overline{a} - E(a) \tag{7}$$

$$\Delta a^{\downarrow} = E(a) - \underline{a} \tag{8}$$

In this paper, the interval formulation above has been considered to model the PV generation and energy price, since these parameters and their corresponding confidence margins can be easily predicted using conventional forecast techniques [31].

3.2 - Utility grid modelling

The utility grid can be simply modelled by the constraints (9) and (10). The former limits the amount of power exchanging while the latter prevents concurrent purchases and sales.

$$p_{r|t}^{Grid,i} \leq u_t^{Grid,i} \cdot \overline{p}^{Grid};\ \forall r \in \mathbb{R} \wedge t \in \mathbb{T} \wedge i \in \{buy, sell\} \tag{9}$$

$$\sum_{i\in\{buy,sell\}}\left\{u_t^{Grid,i}\right\} \leq 1;\ \forall t \in \mathbb{T} \tag{10}$$

On the other hand, it is realistic to assume that the utility grid cannot vary its generation profile quickly, as it is mainly formed by slow-response generators [40]. This restriction is modelled by including ramping limits in (11).

$$p_{r|t-1}^{Grid,buy} - RD^{Grid} \leq p_{r|t}^{Grid,buy} \leq p_{r|t-1}^{Grid,buy} + RU^{Grid};\ \forall r \in \mathbb{R} \wedge t \in \mathbb{T} \backslash t > 1 \tag{11}$$

3.3 - PV modelling

As commented, potential PV generation is modelled as an interval number in this paper according to (5)-(8). The predicted PV generation will limit the amount of energy that PV panels can deliver, which is depicted in the constraint (12).

$$p_{r|t}^{PV} \leq [\hat{p}_t^{PV}];\ \forall r \in \mathbb{R} \wedge t \in \mathbb{T} \tag{12}$$

Indeed, the PV potential generation in (12) has been modelled as an interval number, assuming that it can be day-ahead predicted with sufficient accuracy, which is a feasible adoption [31].

3.4 - Hydrogen chain modelling

The basic formulation of the hydrogen chain considered in this paper was drawn in Section 2.1. However, this modelling considers fast dynamic responses. This formulation can be simplified in energy management problems assuming a sufficiently large time step. This way, the equations (1)-(4) can be linearized [27]. Hence, the hydrogen mass flow in the electrolyser and FC can be calculated by (13) and (14), respectively. On the other hand, the operation of both electrolysers and FCs is subjected to the maximum and minimum dispatchable powers by (15) and ramping restrictions by (16) [5]. Finally, model (17) establishes coherency among the commitment and on/off variables.

$$g_{r|t}^{EZ} = \eta^{EZ} \cdot \frac{p_{r|t}^{EZ}}{\text{LHV}};\ \forall r \in \mathbb{R} \wedge t \in \mathbb{T} \tag{13}$$

$$g_{r|t}^{FC} = \frac{p_{r|t}^{FC}}{\text{LHV} \cdot \eta^{FC}};\ \forall r \in \mathbb{R} \wedge t \in \mathbb{T} \tag{14}$$

$$u_t^i \cdot \underline{p}^i \leq p_{r|t}^i \leq u_t^i \cdot \overline{p}^i;\ \forall r \in \mathbb{R} \wedge t \in \mathbb{T} \wedge i \in \{EZ, FC\} \tag{15}$$

$$p_{r|t-1}^i - RD^i \leq p_{r|t}^i \leq p_{r|t-1}^i + RU^i;\ \forall r \in \mathbb{R} \wedge t \in \mathbb{T} \backslash t > 1 \wedge i \in \{EZ, FC\} \tag{16}$$

$$u_t^i - u_{t-1}^i = \text{on}_t^i - \text{off}_t^i;\ \forall r \in \mathbb{R} \wedge t \in \mathbb{T} \backslash t > 1 \wedge i \in \{EZ, FC\} \tag{17}$$

In this paper, FCEV demand is considered unknown. However, unlike to PV generation and energy pricing, the refuelling demand cannot be easily predicted due to

the high unpredictable driving behaviour [41]. In this sense, the interval notation described in 3.1 is not suitable to model the hydrogen demand and, therefore, this parameter has been modelled via scenarios [42]. The stochastic modelling of FCEV demand will be described in the following section. Herein, only the constraint (18) is provided, which establishes that the amount of hydrogen refuelled cannot exceed expected demand.

$$g_{r|t}^{FCEV} \leq u_{r|t}^{FCEV} \cdot \hat{g}_{r|t}^{FCEV};\ \forall r \in \mathbb{R} \wedge t \in \mathbb{T} \tag{18}$$

To establish a coherent behaviour in the hydrogen chain, it is assumed that FC/compressor is complementary to the electrolyser. In this regard, both devices could not be scheduled at the same time, as established in (19) and (20).

$$\sum_{i\in\{EZ,FC\}}\{u_t^i\} \leq 1;\ \forall t \in \mathbb{T} \tag{19}$$

$$u_t^{EZ} + u_{r|t}^{FCEV} \leq 1;\ \forall r \in \mathbb{R} \wedge t \in \mathbb{T} \tag{20}$$

Finally, the state of pressure in the hydrogen tank is modelled by linearizing (2) and assuming steady-state conditions. Thus, the inflow and outflow mass flows are equal to the hydrogen flows in the electrolyser and the FC/compressor, as said in the model (21), which also considers gas dissipation [27]. Lastly, the constraint (22) limits the pressure of the hydrogen vessels and the Eq. (23) sets the initial and final state of pressure in order to facilitate the scheduling process [5, 27].

$$SOP_{r|t}^{HSS} = SOP_{r|t-1}^{HSS} + \gamma \cdot \frac{\mathcal{R}\cdot\theta^{HSS}}{v^{HSS}\cdot\zeta} \cdot \left(g_{r|t}^{EZ} - g_{r|t}^{FC} - g_{r|t}^{FCEV}\right) \cdot \Delta\tau - \frac{\varrho}{100} \cdot SOP_{r|t-1}^{HSS};\ \forall r \in \mathbb{R} \wedge t \in \mathbb{T} \backslash t > 1 \tag{21}$$

$$\underline{SOP}^{HSS} \leq SOP_{r|t}^{HSS} \leq \overline{SOP}^{HSS};\ \forall r \in \mathbb{R} \wedge t \in \mathbb{T} \tag{22}$$

$$SOP_{r|\mathbb{T}(1)}^{HSS} = SOP_{r|\mathbb{T}(\text{end})}^{HSS} = \overline{SOP}^{HSS};\forall r \in \mathbb{R} \tag{23}$$

3.5 - System balance

Anytime, the power balance in the system must be met. This is ensured by imposing the constraint (24), which also accounts for the power consumption of the compression stages.

$$p_{r|t}^{Grid,buy} + p_{r|t}^{PV} + p_{r|t}^{FC} = p_{r|t}^{Grid,sell} + p_{r|t}^{EZ} + \frac{g_{r|t}^{FCEV} \cdot \varsigma^{Comp}}{\Delta\tau \cdot \eta^{Comp}};\ \forall r \in \mathbb{R} \wedge t \in \mathbb{T} \quad (24)$$

3.6 - System profit

The system operator aims at maximizing his own profit. For the system under study, the monetary balance is expressed as follows,

$$F = F^{FCEV} - F^{Grid} - F^{EZ} - F^{FC} \quad (25)$$

The expression above encompasses different factors that account for the revenues and expenditures of different monetary processes. The first term in (25) expresses the monetary revenues obtained from FCEV refuelling, which are given by (26). The second term accounts for the monetary balance with the utility grid, established by (27). Finally, the last two elements in (25) are the operation and maintenance costs of the electrolyser and FC, which encompass fixed and variable expenditures as said (28) [5].

$$F^{FCEV} = \sum_{r\in\mathbb{R}}\left\{\omega_r \cdot \sum_{t\in\mathbb{T}}\left\{\pi^{FCEV} \cdot g_{r|t}^{FCEV}\right\}\right\} \quad (26)$$

$$F^{Grid} = \sum_{r\in\mathbb{R}}\left\{\omega_r \cdot \Delta\tau \cdot \sum_{t\in\mathbb{T}}\left\{\left[\hat{\lambda}_t^{Grid,buy}\right] \cdot p_{r|t}^{Grid,buy} - \left[\hat{\lambda}_t^{Grid,sell}\right] \cdot p_{r|t}^{Grid,sell}\right\}\right\} \quad (27)$$

$$F^{i} = \sum_{r\in\mathbb{R}}\left\{\omega_r \cdot \sum_{t\in\mathbb{T}}\left\{\Delta\tau \cdot \left(\frac{\kappa^i \cdot \overline{p}^i}{T^i} \cdot u_t^i + p_{r|t}^i \cdot \chi^i\right) + \vartheta^i \cdot \left(\mathrm{on}_t^i + \mathrm{off}_t^i\right)\right\}\right\};\ \forall i \in \{EZ, FC\} \quad (28)$$

It is noteworthy that the energy price of both selling and purchasing processes has been modelled as interval numbers in (27), as previously commented.

4 - Stochastic modelling of the FCEV demand

Unlike to PV generation and energy pricing, FCEV demand is highly unpredictable due to random behaviour of drivers [41]. In this regard, the interval notation considered for the other uncertainties is not suitable in this case, since forecast information is difficult

to obtain. One of the main contributions of this work is to develop a comprehensive stochastic model for FCEV demand. For the sake of clarity, the developed scenario generation process is summarized in the flowchart of Fig. 3 and fully explained below.

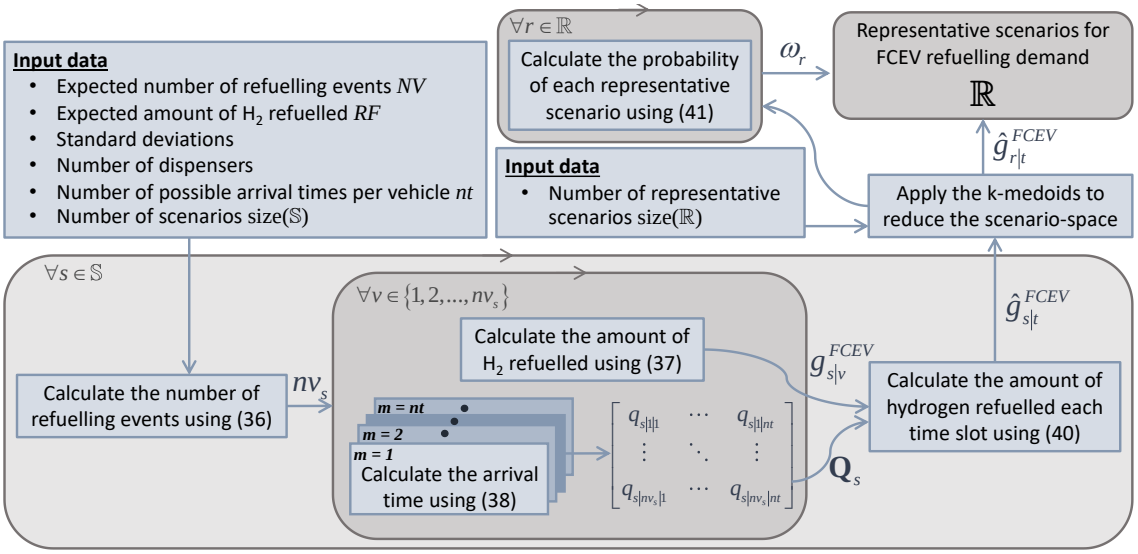

Fig. 3. Flowchart of the developed stochastic modelling for FCEV demand

4.1 - Inputs

Several inputs must be provided to the scenario generator. Firstly, the total number of dispensers is necessary to reproduce realistic results since, otherwise, the FCEV demand may be overestimated. Secondly, the expected number of events and hydrogen refuelled per event must be provided. These two parameters can be easily approximated. In the case of refuelling events, it can be set based on historical data or reports, while the total amount of hydrogen refuelled per event can be estimated on the basis of the average capacity of current vehicle models (~5 kg [14]). Finally, the number of scenarios together with the number of time arrivals per vehicle define the size of the scenario-space. These parameters can be freely set for convenience; however, it is recommended to generate a large number of scenarios to produce reliable results (e.g. ~1,000 [43]).

4.2 - Modelling the driving behaviour

According to [44], the daily mileage of FCEVs can be approximated by a Gamma distribution. In [45], this Gamma distribution is fitted according to real data, taking 15 and 1.4 as the most frequent values for the scale and shape parameters, respectively. Assuming these parameters, the probability distribution function for the FCEVs daily mileage is given by

$$\mathfrak{W}(y) = \frac{y^{0.4} \cdot e^{\left(-y/15\right)}}{44.31 \cdot \Gamma(1.4)} \tag{29}$$

As in [41], instead of considering all the possible mileages within the interval $[y_j, y_{j+1})$, the average mileage, namely y_k calculated in (30), is used as an indicator. Thus, the probability of y_k mileage can be obtained by (31).

$$y_k = \frac{1}{2} \cdot \left(y_j + y_{j+1}\right) \tag{30}$$

$$W(y_k) = \int_{y_j}^{y_{j+1}} w(y)dy \tag{31}$$

The vehicle trip distribution draws the probability of a FCEV is driving on the road at time t. This distribution is publicly available in [46] and is plotted in Fig. 4. If the vehicle trip distribution is denoted by $\mathfrak{O}(t)$, being therefore the probability for a particular time instant namely t_i equals to $O(t_i)$, the probability of a vehicle drives y_k mileages at time t_i can be calculated as

$$D(y_k, t_i) = W(y_k) \cdot O(t_i) \tag{33}$$

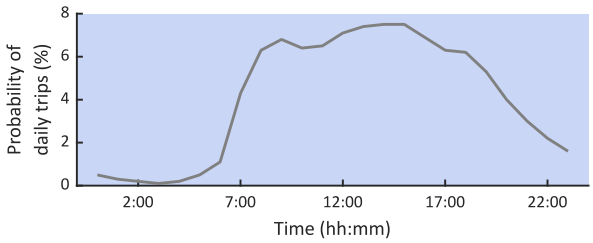

Fig. 4. Vehicle trip distribution (taken from [46])

Taking size($\mathbb{T}$) time intervals for convenience and n different mileages, the distribution yielded by (33) can be arranged in matrix form, as follows

$$\mathbf{D} = \begin{bmatrix} D\left(y_1, \mathbb{T}(1)\right) & \dots & D\left(y_n, \mathbb{T}(1)\right) \\ \vdots & \ddots & \vdots \\ D\left(y_1, \mathbb{T}(\text{end})\right) & \dots & D\left(y_n, \mathbb{T}(\text{end})\right) \end{bmatrix} \in \mathbb{R}^{\text{size}(\mathbb{T}) \times n} \tag{33}$$

Therefore, the matrix (33) gives the probability of a FCEV is driving y_k mileages at t_i time instant. Intuitively, the probability that a vehicle will actually refuel depends on the distance driven by the vehicle. In other words, it is more probable that a given vehicle will refuel if it drives large distances. Currently, the autonomy of FCEVs ranges from 300 to 500 miles [7, 46]. In this paper, the probability of refuelling is assumed to grow with the driven mileage according to the following distribution

$$\phi(y) = \begin{cases} \frac{e^{0.01 \cdot y} - e^{0.01}}{e^{2.49} - e^{0.01}}, & \text{for } 1 \leq y \leq 249 \\ 1, & \text{for } 250 \leq y \leq 300 \end{cases} \tag{34}$$

Indeed, following (34) the probability of refuelling grows exponentially with the driven mileage. It is worth noting that (34) considers that a vehicle will refuel with total probability if it is driven more than 250 miles.

4.3 - Modelling the hydrogen refuelled probability

Once (34) has been calculated for n different mileages, the probability of refuelling at any time instant can be calculated as follows

$$\boldsymbol{h} = \mathbf{D} \cdot \boldsymbol{\phi}^{\mathrm{T}} \rightarrow \mathfrak{G}(t) \tag{35}$$

Hence, the probability distribution $\mathfrak{G}(t)$ will yield the probability of refuelling event as a function of the driven mileages and probability of a vehicle is driving on road at any time instant.

4.4 - Calculating the FCEV demand

Once the expected number of refuelling events (denoted by NV) has been estimated, the actual number of refuelling events for the s^{th} scenario can be calculated using a fitted Gaussian distribution, as follows,

$$nv_s = \text{round}\left(\text{rand}\left(\mathfrak{N}(NV, \sigma_{NV})\right)\right);\ \forall s \in \mathbb{S} \tag{36}$$

Likewise, the expected hydrogen refuelled by the v^{th} vehicle (or refuelling event) of the s^{th} scenario can be approximated by a normal distribution as follows,

$$g_{s|v}^{FCEV} = \text{round}\left(\text{rand}\left(\mathfrak{N}(RF, \sigma_{RF})\right)\right);\ \forall s \in \mathbb{S} \wedge v \in \{1,2,\dots,nv_s\} \tag{37}$$

It is noteworthy that (36) and (37) assumes that Gaussian distributions are good representations of the concerned parameters, which is reasonable for those unknowns whose mean and standard deviation can be easily estimated [27]. The arrival time will be a function of the probability of refuelling event at any time instant, which can be approximated by $\mathfrak{G}(t)$. In this paper, nt different time arrivals are considered for each vehicle, therefore

$$q_{s|v|m} = \text{round}\left(\text{rand}(\mathfrak{G})\right);\ \forall s \in \mathbb{S} \wedge v \in \{1,2,\dots,nv_s\} \wedge m \in \{1,2,\dots,nt\} \tag{38}$$

At this point, if the total number of vehicles that will refuel at a given time instant is higher than the number of available dispensers, it is assumed that the excess of refuelling events is lost since the station has not the capacity to satisfy this demand (note that this step has been omitted in Fig. 3 for simplicity). The nt different time arrivals considered for each of the nv_s in the s^{th} are arranged in matrix form, as follows

$$\boldsymbol{Q}_s = \begin{bmatrix} q_{s|1|1} & \cdots & q_{s|1|nt} \\ \vdots & \ddots & \vdots \\ q_{s|nv_s|1} & \cdots & q_{s|nv_s|nt} \end{bmatrix} \in \mathcal{Z}^{nv_s \times nt};\ \forall s \in \mathbb{S} \tag{39}$$

The matrix (39) allows to easily calculate the instantaneous hydrogen demand using (40). Note that different time resolutions can be used for the stochastic modelling and the scheduling tool. This is very suitable since, while a hydrogen refuelling event takes very short times (~5 min), energy management tools may eventually use larger time resolutions (≥ 15 min).

$$\hat{g}_{s|t}^{FCEV} = \sum_{v \in \{q_{s|v|m} == t\}} \left\{ g_{s|v}^{FCEV} \right\};\ \forall s \in \mathbb{S} \wedge m \in \{1,2,\dots,nt\} \tag{40}$$

As a sake of example, Fig. 5 shows various demand profiles generated by the developed stochastic model. In this case, the number of dispensers has been considered absurdly high for illustrative purposes.

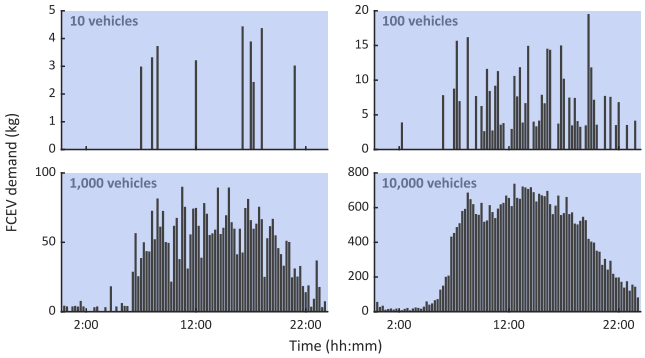

Fig. 5. Examples of FCEV demand scenarios generated with the developed stochastic model

4.5 - Data reduction

The number of scenarios to be generated is normally very large, which may result in intractable optimization procedures. To overcome this issue, clustering techniques can be used [47]. These methods reduce the scenario-space to a minimal set of representative profiles. This way, the representative scenarios are considered to be an accurate, but reduced representation of the whole scenario-space. In this paper, the k-medoids method has been considered because of its overall good features [48]. Once the representative scenarios have been obtained, the probability of each scenario can be calculated by

$$\omega_r = \frac{\text{size}(\boldsymbol{\Omega}_r)}{\text{size}(\mathbb{S})};\ \forall r \in \mathbb{R} \tag{41}$$

5 - Solution methodology

To solve the optimization problem described in Section 3 using interval formulation and stochastic modelling of FCEV demand, an iterative procedure is proposed, which is summarized in Fig. 6. In essence, the developed methodology raises a multi-stage procedure that allows to adopt different operational strategies [49]. On the one hand, the risk-averse perspective assumes unfavourable behaviour of uncertainties. It means that the value of the unknown parameters impacts negatively on the monetary profit. For

example, the PV generation presumably take values in the lower section of its predicted interval; thus, the system will be forced to purchase more energy from the grid and therefore the monetary expenditures will grow. In contrast, under a risk-seeker strategy, the uncertainties will take favourable profiles.

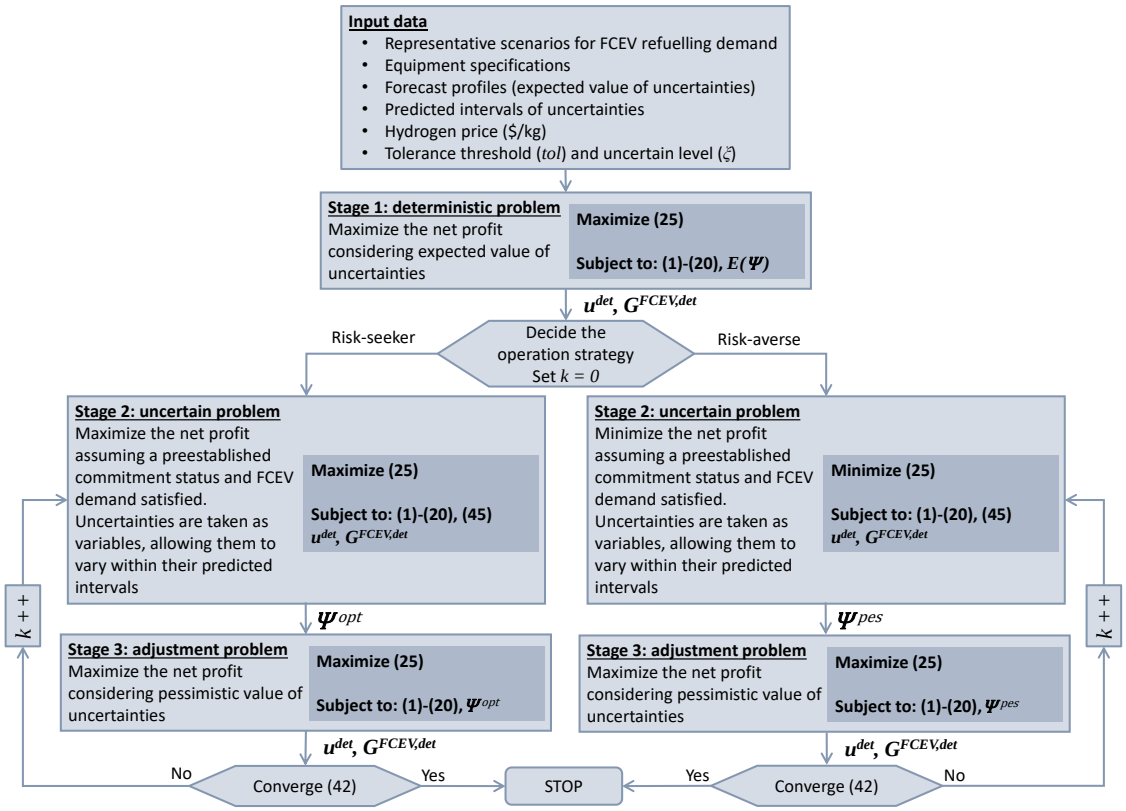

Fig. 6. Flowchart of the developed solution procedure

Once the strategy has been decided, different stages are iteratively solved until the uncertainty-aware scheduling result is obtained. This scheduling plan will be immune against possible deviations of uncertainties with respect to their expected values [50]. Subsequent sections are devoted to explain each stage in depth. The iterative procedure will stop when two consecutive solutions do not differ substantially, which can be established by

$$\frac{\left|F_k^{(3)} - F_k^{(2)}\right|}{F_k^{(3)}} \leq tol \tag{42}$$

where tol is a predefined convergence tolerance (0.01 in this paper), the subscripts denote the k^{th} iteration, and the superscripts indicate the stage number.

5.1 - Stage 1: deterministic problem

At Stage 1, the problem is solved from a deterministic point of view. In this sense, FCEV demand is the unique uncertainty which is modelled via scenarios. Therefore, the different uncertainties that are modelled as interval numbers (PV generation and energy pricing) are assumed to take their expected values. Thereby, the Stage 1 can be formulated as

$$\boldsymbol{u}^{det}, \boldsymbol{G}^{FCEV,det} \rightarrow \underset{\boldsymbol{x},\boldsymbol{u}}{\operatorname{argmax}} F\big(E(\boldsymbol{\Psi})\big) \tag{43}$$

Subject to: (1)-(20)

where

$$\boldsymbol{G}^{FCEV,det} = \begin{bmatrix} g^{FCEV}_{\mathbb{S}(1)|\mathbb{T}(1)} & \cdots & g^{FCEV}_{\mathbb{S}(1)|\mathbb{T}(\text{end})} \\ \vdots & \ddots & \vdots \\ g^{FCEV}_{\mathbb{S}(\text{end})|\mathbb{T}(1)} & \cdots & g^{FCEV}_{\mathbb{S}(\text{end})|\mathbb{T}(\text{end})} \end{bmatrix} \in \mathcal{R}_{+}^{\text{size}(\mathbb{S})\times\text{size}(\mathbb{T})} \tag{44}$$

5.2 - Stage 2: uncertain problem

Stage 2 is devoted on seeking the most unfavourable/favourable value of uncertainties for which the problem is still feasible. To this end, the commitment results and actual FVEV demand satisfied are assumed to be imposed by the deterministic problem. At this stage, the uncertainties are taken as decision variables, which can vary within their predicted intervals, as said the constraint (45).

$$E(a) - \xi \cdot \Delta a^{\downarrow} \leq a \leq E(a) + \xi \cdot \Delta a^{\uparrow}; \forall a \in \boldsymbol{\Psi} \tag{45}$$

In (45), $\xi \in [0,1]$ is the so-called uncertain level [5], which allows to set the degree of robustness of the algorithm. Thus, the problem can turn more uncertain-oriented or more deterministic depending on the value of ξ. For example, if $\xi = 1$, the interval is fully considered in (45), while $\xi = 0$ becomes the problem deterministic.

According to the premises above, the Stage 2 can be mathematically stated as follows

$$\boldsymbol{\Psi}^{opt} \rightarrow \underset{\boldsymbol{x},\boldsymbol{\Psi}}{\text{argmax}}\, F(\boldsymbol{u}^{det}, \boldsymbol{G}^{FCEV,det}) \tag{46a}$$

$$\boldsymbol{\Psi}^{pes} \rightarrow \underset{\boldsymbol{x},\boldsymbol{\Psi}}{\text{argmin}}\, F(\boldsymbol{u}^{det}, \boldsymbol{G}^{FCEV,det}) \tag{46b}$$

Subject to: (1)-(20), (45)

5.3 - Stage 3: adjustment problem

Once the pessimistic/optimistic profiles of uncertainties have been calculated at Stage 2, it is necessary to adjust the scheduling result according to the new profiles, which is performed at Stage 3 by solving the following optimization problem.

$$\boldsymbol{u}^{det}, \boldsymbol{G}^{FCEV,det} \rightarrow \underset{\boldsymbol{x},\boldsymbol{u}}{\text{argmax}}\, F\left(\boldsymbol{\Psi}^{i}\right); i \in opt \vee pes \tag{47}$$

Subject to: (1)-(20)

6 - Case study

This section presents a case study based on the benchmark installation described in Section 2. The described MILP + QP optimization framework can be easily addressed by conventional solvers. In particular, the mathematical models were written in Matlab R2020b using a friendly model-based code using Gurobi [51], which is currently freely available for research and academic purposes. The simulations were run on an Intel® CoreTM i7-10700K CPU 3.80GHz 3.79 GHz personal computer over 24 h time horizon with 15 min resolution. Experiments carried out by the authors consumed 15-30 minutes on average, which is reasonable for energy management tools [52]. In addition, its MILP + QP structure ensures a good scalability to larger systems [53].

6.1 - Data

It is assumed that the installation under study is connected to an upscale grid that is managed by a local utility company. The station can exchange up to 500 kW with the upscale network, which admits ramps of 300 kW. Fig. 7 plots the expected PV generation and energy pricing. The solar potential has been constructed based on the irradiance and

temperature observed in Madrid (Spain) on July 19, 2016 [54], considering a PV array of 250 kWp. On the other hand, the purchasing energy price corresponds with the real-time price at the PJM FE Ohio system on July 1, 2019 [55], while the selling price has been taken 0.6 times the purchasing cost, as customary [56]. Other relevant data regarding the hydrogen chain are collected in Table 3.

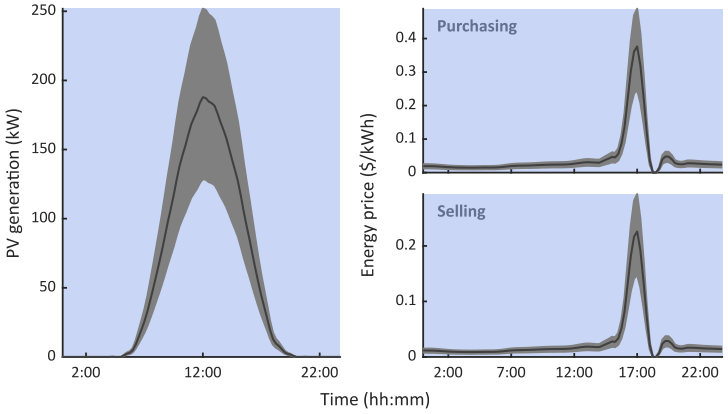

Fig. 7. Expected PV generation and energy pricing

Table 3. Hydrogen chain data [5, 20, 27, 58]

Parameter	Value	Parameter	Value
$\underline{p}^{EZ}/\overline{p}^{EZ}$	400/25 kW	v^{HSS}	200 m³
$\underline{p}^{FC}/\overline{p}^{FC}$	400/25 kW	θ^{HSS}	313 K
RU^{EZ}/RD^{EZ}	300 kW	γ	0.0001
RU^{FC}/RD^{FC}	300 kW	$\mathcal{R}$	8.314 J/K·mol
$\eta^{EZ}/\eta^{FC}/\eta^{Comp}$	0.65/0.77/0.8 p.u.	ζ	0.002 kg/mol
κ^{EZ}/κ^{FC}	8.5/32 $/kW	ϱ	0.006 %
T^{EZ}/T^{FC}	10,000 hrs	LHV	39.72 kWh/kg
$\vartheta^{EZ}/\vartheta^{FC}$	0.15/0.02 $	ς^{Comp}	2.7 kWh/kg
χ^{EZ}/χ^{FC}	0.03 $/kWh	$\underline{SOP}^{HSS}/\overline{SOP}^{HSS}$	2/10 bar

Nowadays, FCEV refuelling price ranges from 7 to 13 $/kg, depending on the country [57]. However, some recent studies pointed out that this price should be notably reduced to be competitive with battery and hybrid vehicles [59]. In this regard, a refuelling price of 2 $/kg has been taken, assuming this cost as the most probable in a future scenario with high penetration of FCEVs. On the other hand, a medium-scale PVaRFS has been considered with 15 dispensers in total. Based on these parameters and assuming common

characteristics of current commercial vehicles, 1,000 demand scenarios have been constructed assuming $\sigma_{NV} = 5$ and $\sigma_{RF} = 1$. Posteriorly, the scenario-space was reduced to 10 representative profiles following the procedure described in Section 5.

6.2 - Results: deterministic case

First, the deterministic case is analysed. This problem corresponds with the Stage 1 of the developed procedure, in which only the FCEV demand is unknown. Fig. 8 shows the scheduling result for this scenario considering $NV = 40$. As observed in this figure, both the electrolysers and compressors are mostly operated to keep the state of pressure within acceptable margins and thus satisfy the FCEV demand. However, at 17:00 h the FCs are operated to sell back energy to the grid. This is due to at this hour the selling price is high. Hence, the hydrogen stored can be managed to supply FCs and obtain a monetary revenue. This result evidences that PVaRFSs can be exploited as electric generators, thus improving its economy.

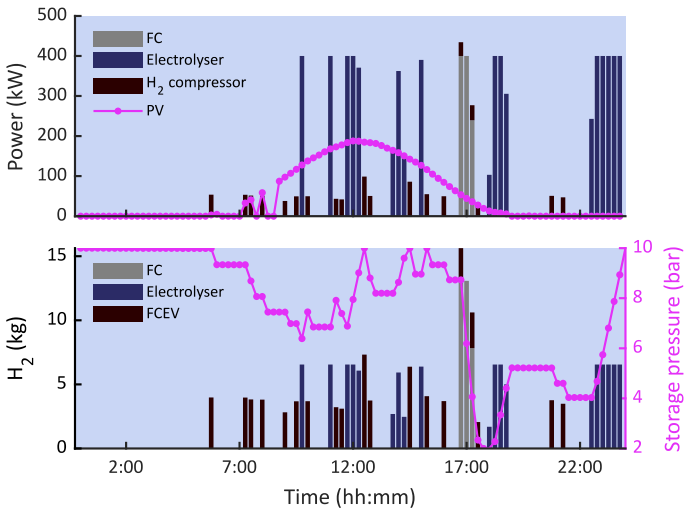

Fig. 8. Scheduling result at Stage 1 with $NV = 40$

Nevertheless, FCEV refuelling supposes the main monetary profit for the installation. This is evident analysing the Fig. 9, where different monetary indicators are shown for various expected refuelling events (NV). As expected, monetary incomes due to FCEV demand grows with NV. Actually, the expected profit raised from ~83 $ to ~228 $ when

the expected number of refuelling events varies from 20 to 100. However, the revenue for energy selling and satisfied demand are both clearly reduced, observing a reduction by 74% and 32% in both indicators, respectively. This is due to the capacity of the station is not sufficient to cover the FCEV demand. In the face of this situation, the system needs to dedicate more energy to satisfy the hydrogen demand, which hinders the capability to send energy to the grid. Likewise, more refuelling events are lost due to the capacity of the HSS is compromised.

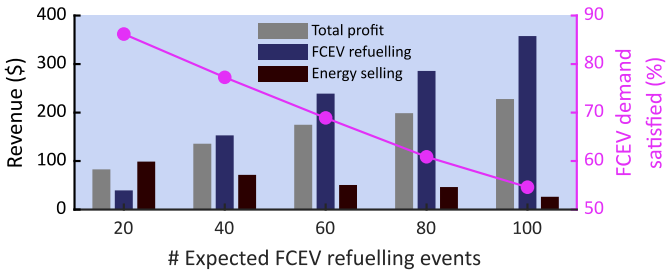

Fig. 9. Indicators obtained for different expected refuelling events at Stage 1

6.3 - Interval analysis

Now, uncertainty regarding PV generation and energy pricing is incorporated via interval analysis. In this sense, different strategies can be adopted, producing different results. This is clearly illustrated in Fig. 10, where the total profit is plotted for different values of NV and ξ. In the case of adopting a risk-seeker strategy, the total profit grows with both parameters. Nonetheless, the profit still rises with NV under a risk-averse strategy; however, the revenue is clearly reduced with the uncertain level. This is due to the expected number of refuelling events impacts positively on the objective function regardless of the strategy adopted. In contrast, the uncertain level measures the degree in which the uncertainties can deviate from their expected profiles. This way, unknowns increase their impact on the monetary revenues with the value of ξ. For example, if $\xi = 1$, the PV generation is allowed to hit the upper limit of its predicted interval; however, if $\xi = 0.2$, the interval can only be considered by 20%. Thus, the influence of the uncertain

level will be positive when adopting a risk-seeker strategy and negative under a risk-averse scheme. This is more clearly observed in Fig. 11, where the scheduling result with both strategies is plotted. As observed, the PV generation increases under a risk-seeker strategy in comparison with its expected profile, while the opposite was observed under a risk-averse strategy. In the simulations performed, variations up to 56% of the expected profit were observed depending on the strategy adopted. In particular, the expected profit fell from ~228 $ in the deterministic case to ~215 $ when adopting a risk-averse strategy, while it increases to ~262 $ in case of assuming a risk-seeker point of view.

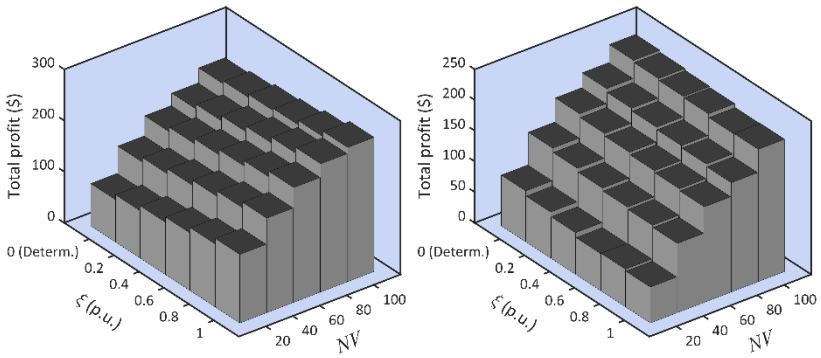

Fig. 10. Total profit assuming risk-seeker (left) and risk-averse (right) strategies

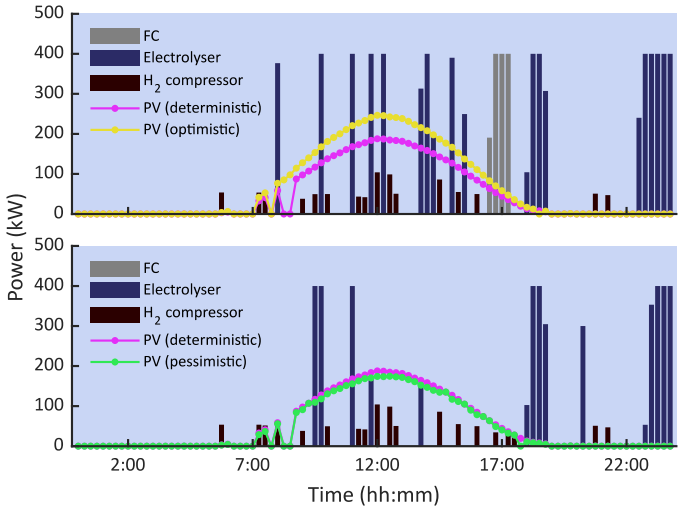

Fig. 11. Scheduling result at Stage 3 with $NV = 40$ and $\xi = 1$ assuming a risk-seeker (top) or risk-averse (bottom) strategy

Obviously, the strategy adopted affects the final scheduling result. This is evident in Fig. 11, where the FCs were not operated when a risk-averse strategy was adopted. This is due to two reasons, on the one hand, the PV generation and selling price are lower,

while on the other hand the buying pricing is higher compared to the expected profiles in the case of risk-averse strategy. These trends impact on the monetary balances of the installation. Figs. 12-14 show different monetary indicators depending on the value of NV and ξ. As seen, the refuelling profit always increases with NV, as expected. However, this indicator is slightly reduced with ξ regardless of the strategy adopted, descending from ~358 $ to ~331 $ in case of adopting a risk-seeker strategy. It means that monetary incomes due to FECV refuelling decreases with the uncertain level, even adopting a risk-seeker strategy, which was not expected. This result is better explained by observing Fig. 13, where the total revenues from energy selling are shown. As observed, this indicator falls with both NV and ξ, but it is considerably lower in case of assuming a risk-averse strategy. Therefore, the operational strategy impacts more notably on the revenues obtained from selling energy rather than on the FCEV profit. This is explained in the fact that, when uncertainties impact negatively, the scheduling tool prioritizes the satisfaction of FCEV refuelling events, from which a high profit can be obtained, while energy selling is only attractive with high PV penetration and selling pricing. In fact, the energy selling revenue may vary up to 85% depending on the strategy adopted, while the FCEV profit scarcely varies by 15%. This operational principle is better observed in Fig. 14, where the total purchasing cost is plotted for different cases. As seen in this figure, these expenditures hardly vary with the strategy adopted (~1%). It means that the total energy purchased scarcely differs between strategies and therefore the unique difference is the usage of the acquired energy. Thus, in case of taking risk-seeker point of view, a considerable portion of the purchased energy is dedicated on be sold back to the grid (~16%), which is an attractive economic activity propitiated by high PV generation and selling prices. In contrast, these uncertainties vary negatively in case of adopting a risk-averse strategy, which makes economically inviable the selling process.

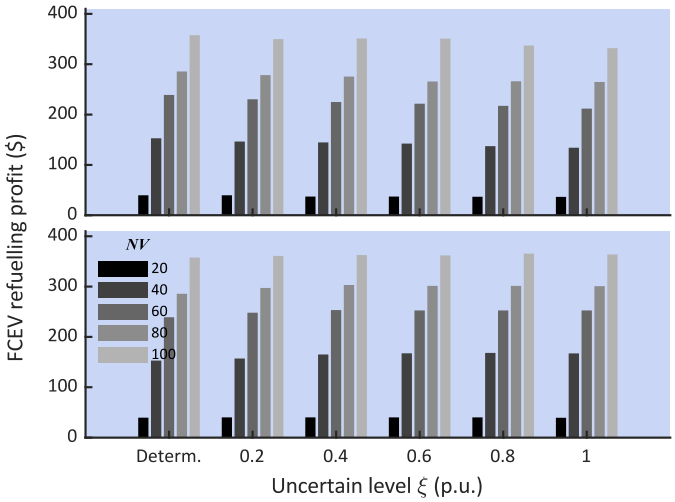

Fig. 12. Total FCEV refuelling profit depending on NV and ξ adopting a risk-seeker (top) or risk-averse (bottom) strategy

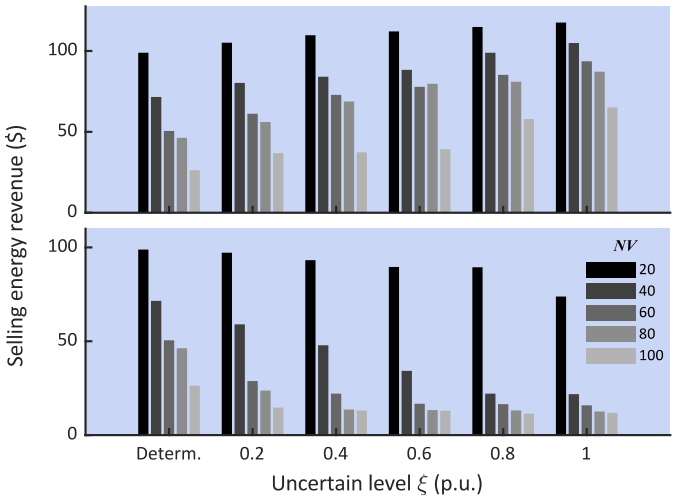

Fig. 13. Total selling energy revenue depending on NV and ξ adopting a risk-seeker (top) or risk-averse (bottom) strategy

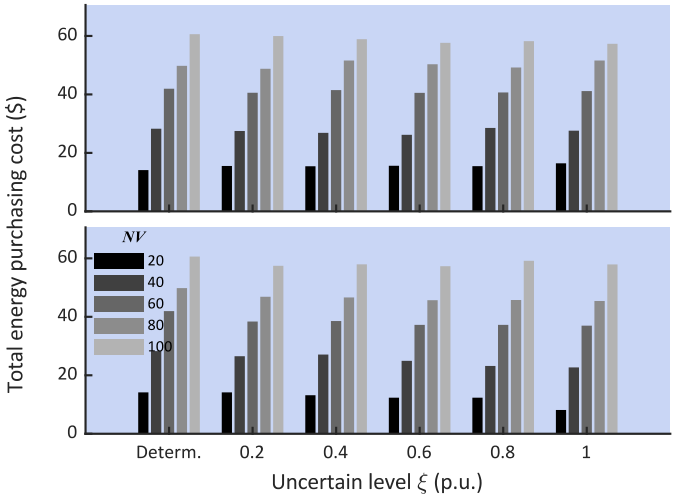

Fig. 14. Total purchasing energy cost depending on NV and ξ adopting a risk-seeker (top) or risk-averse (bottom) strategy

Finally, it is worth analysing the effect of uncertainties in energy prices. Fig. 15 compares the average purchasing and selling prices for different cases. As observed, the purchasing price decreases with the uncertain level in case of adopting a risk-seeker strategy, whereas the selling price grows. In contrast, the opposite trend is followed under a risk-averse perspective. These results stand out how the different operational strategies affect to expected profiles in energy costs. Thus, the selling price is assumed to be higher in case of adopting a risk-seeker strategy, since in this case the operator seeks to maximize his own profit at expenses on assuming more risk. Under this perspective, the selling price is assumed to vary positively in comparison with its expected profile, while the opposite behaviour is observed under a risk-averse point of view. This trend makes more attractive selling energy to the grid, encouraging to deliver more energy as the uncertain level grows, as observed in Fig. 13.

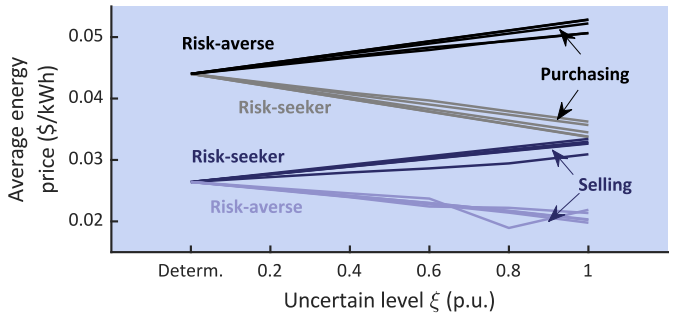

Fig. 15. Average purchasing and selling prices under different operational strategies

6.4 - Comparison with fully stochastic programming

A wide variety of uncertainties modelling is available in the literature, ranging from Montecarlo simulation to fully robust optimization [60]. Among them, maybe the most widely used is stochastic programming. This approach is very useful for those uncertainties whose probability distribution is known or historical data is available. This modelling has been used in this paper for FCEV demand, while interval notation was considered for PV generation and energy pricing. However, the developed formulation

could be adapted to fully stochastic programming without difficulty. This section focuses on comparing the new proposal with the conventional stochastic programming. To do that, Gaussian distribution of forecast errors has been assumed, as usual [27]. In order to provide a faith comparison, the same number of representative scenarios were generated using the data reduction technique detailed in Section 4.5.

The first main difference arises in the fact that only a risk-seeker strategy can be adopted in case of stochastic programming, which suppose a clear advantage of interval notation. As seen in Fig. 16, where the objective function (profit) is compared considering fully stochastic programming and the developed methodology, the developed method always yields a more conservative profit in case of adopting a risk-seeker strategy. This is due to stochastic programming calculates the average objective function among scenarios, regardless they are unfavourable or not, while interval notation seeks for the most unfavourable profile for uncertainties. As expected, the profit obtained under a risk-seeker strategy was considerably higher compared with stochastic programming. Fig. 15 also reports the average execution time. In this case, differences were marginal. However, the overall computational effort in case of stochastic programming is expected to be higher if the scenario generation process is considered. This is due to the necessity of generating scenarios for PV generation and energy pricing as well, which is more time consuming than simply adding confidence intervals on forecast profiles.

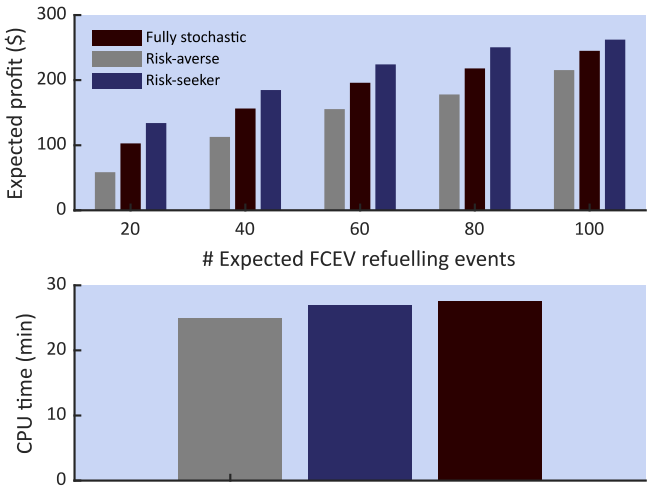

Fig. 16. Expected profit and CPU time using the developed procedure and fully stochastic programming ($\xi = 1$)

7 - Conclusions

A novel stochastic-interval model has been developed for energy management in PVaRFSs. The new proposal takes advantage of different models to properly handle heterogeneous uncertainties in this kind of infrastructures. Thus, while the PV generation and energy pricing are modelled using interval notation, the FCEV demand has been treated using scenarios. To this end, a comprehensive stochastic modelling for refuelling demand has been developed based on reported driving behaviour and common characteristics of commercial vehicles. As result, a novel stochastic-interval approach is obtained, which has been used for the first time in PVaRFSs. An iterative solution procedure has been developed for the proposed model, which allows, in contrast to other uncertainties modelling, to adopt and analyse risk-seeker and risk-averse strategies, thus supposing a valuable tool to evaluate the viability of PVaRFSs.

Extensive simulations have been performed on a benchmark PVaRFS. The results obtained allow to conclude that:

- Even taking prospective low hydrogen prices, FCEV refuelling is by far the most attractive activity of the station. In all studied cases, revenues obtained from this

activity supposing a large portion of the total incomes, reaching up to 100% of revenues in some cases. Nevertheless, this aspect strongly depends on the expected number of refuelling events.

- In the case study, refuelling events were partially not covered when the expected number of vehicles is high, due to the limited capacity of the station. This evidences the necessity of properly planning the installation, with the object of satisfying as many refuelling events as possible thus maximizing the economic revenues from the main monetary activity of the station.
- Expected profit highly vary depending on the operational strategy and level of uncertainty. In this sense, variations up to 50% were observed depending on the strategy adopted, while the level of uncertainty impacted notably varying the total profit by 40%. This result evidences the necessity of properly evaluating the risk involved in the operation and actuate in consequence.
- Producing electricity through FCs to sell energy was an ideal complement to FCEV refuelling, even supposing the main economic activity when few refuelling events are expected. However, this activity is highly influenced by the level of uncertainty and strategy adopted, observing variations up to 85%.

As deduced from the conclusions above, alternative activities like energy selling may result attractive only when PV generation is high and energy pricing takes favourable values. This is due to the characteristic low efficiency of the hydrogen chain, which requires high jumps between low and peak prices to compensate losses. In this regard, investments in auxiliary equipment like FCs must be carefully evaluated. We hope that the developed tool helps in the task of analysing the viability of PVaRFSs projects. Alternatively, future works will be focused on analysing the viability of hybrid stations, which encompass charging points for pure-electric vehicles and dispensers for FCEVs.

To this end, the developed tool is expected to be very useful, being just necessary to introduce minor modifications.

Acknowledgments

The icons used in this paper were developed by Freepik, Smashicons, surang, AmethystDesign, and Backwoods from www.flaticon.com.

References

[1] C. Gaete-Morales, A. Gallego-Schmid, L. Stamford, A. Azapagic. Life cycle environmental impacts of electricity from fossil fuels in Chile over a ten-year period. *Journal of Cleaner Production* 2019; 232: 1499-1512. https://doi.org/10.1016/j.jclepro.2019.05.374.

[2] J. Li, J. Jiao, Y. Tang. An evolutionary analysis on the effect of government policies on electric vehicle diffusion in complex network. *Energy Policy* 2019; 129: 1-12. https://doi.org/10.1016/j.enpol.2019.01.070.

[3] European Commission. Regulation (EU) 2019/631 of the European Parliament and of the Council of 17 April 2019 setting CO_2 emission performance standards for new passenger cars and for new light commercial vehicles. 2019.

[4] International Energy Agency. Trends and developments in electric vehicle markets. 2021. Online, available at: https://www.iea.org/reports/global-ev-outlook-2021/trends-and-developments-in-electric-vehicle-markets, (accessed Feb. 17, 2022).

[5] M. Tostado-Véliz, S. Kamel, H.M. Hasanien, R.A. Turky, F. Jurado. A mixed-integer-linear-logical programming interval-based model for optimal scheduling of isolated microgrids with green hydrogen-based storage considering demand response. *Journal of Energy Storage* 2022; 48: 104028. https://doi.org/10.1016/j.est.2022.104028.

[6] U.S. Department of Energy. Alternative Fuels Data Center - Fuel Cell Electric Vehicles. Online, available at: https://afdc.energy.gov/fuels/hydrogen.html, (accessed Feb. 17, 2022).

[7] National Renewable Energy Laboratory. Fuel Cell Electric Vehicle Composite Data Products. Online, available at: https://www.nrel.gov/hydrogen/fuel-cell-electric-vehicle-cdps.html, (accessed May 11, 2022).

[8] International Energy Agency. Global EV Outlook 2021. 2021. Online, available at: https://www.iea.org/reports/global-ev-outlook-2021, (accessed Feb. 17, 2022).

[9] H. Blanco, J.J.G. Vilchez, W. Nijs, C. Thiel, A. Faaij. Soft-linking of a behavioral model for transport with energy system cost optimization applied to hydrogen in EU. *Renewable & Sustainable Energy Reviews* 2019; 115: 109349. https://doi.org/10.1016/j.rser.2019.109349.

[10] R. Berger. Hydrogen transportation - The key to unlocking the clean hydrogen economy. 2021. Online, available at: https://www.rolandberger.com/, (accessed Feb. 17, 2022).

[11] H. Tebibel. Methodology for multi-objective optimization of wind turbine/battery/electrolyzer system for decentralized clean hydrogen production using an adapted power management strategy for low wind speed conditions. *Energy Conversion & Management* 2021; 238: 114125. https://doi.org/10.1016/j.enconman.2021.114125.

[12] A.R. Jordehi, M.S. Javadi, J.P.S. Catalão. Day-ahead scheduling of energy hubs with parking lots for electric vehicles considering uncertainties. *Energy* 2021; 229: 120709. https://doi.org/10.1016/j.energy.2021.120709.

[13] S. Carr, F. Zhang, F. Liu, Z. Du, J. Maddy. Optimal operation of a hydrogen refuelling station combined with wind power in the electricity market. *International Journal of Hydrogen Energy* 2016; 41(46): 21057-66. https://doi.org/10.1016/j.ijhydene.2016.09.073.

[14] U. Mukherjee, A. Maroufmashat, A. Narayan, A. Elkamel, M. Fowler. A Stochastic Programming Approach for the Planning and Operation of a Power to Gas Energy Hub with Multiple Energy Recovery Pathways. *Energies* 2017; 10: 868. https://doi.org/10.3390/en10070868.

[15] M. Gökçek, C. Kale. Optimal design of a Hydrogen Refuelling Station (HRFS) powered by Hybrid Power System. *Energy Conversion & Management* 2018; 161: 215-24. https://doi.org/10.1016/j.enconman.2018.02.007.

[16] D. Emad, M.A. El-Hameed, A.A. El-Fergany. Optimal techno-economic design of hybrid PV/wind system comprising battery energy storage: Case study for a remote area. *Energy Conversion & Management* 2021; 249: 114847. https://doi.org/10.1016/j.enconman.2021.114847.

[17] M. Gökçek, C. Kale. Techno-economical evaluation of a hydrogen refuelling station powered by Wind-PV hybrid power system: A case study for İzmir-Çeşme. *International Journal of Hydrogen Energy* 2018; 43(23): 10615-25. https://doi.org/10.1016/j.ijhydene.2018.01.082.

[18] C. Wilke, A. Bnesmann, S. Martin, A. Utz, R. Hanke-Rauschenbach. Optimal design of a district energy system including supply for fuel cell electric vehicles. *Applied Energy* 2018; 226: 129-44. https://doi.org/10.1016/j.apenergy.2018.05.102.

[19] A. Kovač, M. Paranos. Design of a solar hydrogen refuelling station following the development of the first Croatian fuel cell powered bicycle to boost hydrogen urban mobility. *International Journal of Hydrogen Energy* 2019; 44(20): 10014-22. https://doi.org/10.1016/j.ijhydene.2018.11.204.

[20] F. Garcia-Torres, D.G. Vilaplana, C. Bordons, P. Roncero-Sánchez, M.A. Ridao. Optimal Management of Microgrids With External Agents Including Battery/Fuel Cell Electric Vehicles. *IEEE Transactions on Smart Grid* 2019; 10(4): 4299-308. https://doi.org/10.1109/TSG.2018.2856524.

[21] M. Tostado-Véliz, P. Arévalo, F. Jurado. A comprehensive electrical-gas-hydrogen Microgrid model for energy management applications. *Energy Conversion & Management* 2021; 228: 113726. https://doi.org/10.1016/j.enconman.2020.113726.

[22] A. Dadkhah, D. Bozalakov, J.D.M. De Kooning, L. Vandevelde. On the optimal planning of a hydrogen refuelling station participating in the electricity and balancing markets. *International Journal of Hydrogen Energy* 2021; 46(2): 1488-500. https://doi.org/10.1016/j.ijhydene.2020.10.130.

[23] A. Mansour-Satloo et al. A hybrid robust-stochastic approach for optimal scheduling of interconnected hydrogen-based energy hubs. *IET Smart Grid* 2021; 4(2): 241-54. https://doi.org/10.1049/stg2.12035.

[24] T.R. Ayodele, T.C. Moselthe, A.A. Yusuff, M. Ntombela. Optimal design of wind-powered hydrogen refuelling station for some selected cities of South Africa. *International Journal of Hydrogen Energy* 2021; 46(49): 24919-30. https://doi.org/10.1016/j.ijhydene.2021.05.059.

[25] A. Mansour-Satloo et al. Multi-objective IGDT-based scheduling of low-carbon multi-energy microgrids integrated with hydrogen refueling stations and electric vehicle parking lots. *Sustainable Cities & Society* 2021; 74: 103197. https://doi.org/10.1016/j.scs.2021.103197.

[26] M. Agabalaye-Rahvar, A. Mansour-Satloo, M.A. Mirzaei, N. Mohammadi-Ivatloo, K. Zare. Economic-environmental stochastic scheduling for hydrogen storage-based smart energy hub coordinated with integrated demand response program. *International Journal of Energy Research* 2021; 45(14): 20232-57. https://doi.org/10.1002/er.7108.

[27] M.M. Lakouraj, H. Niaz, J.J Liu, P. Siano, A. Anvari-Moghaddam. Optimal risk-constrained stochastic scheduling of microgrids with hydrogen vehicles in real-time and day-ahead markets. *Journal of Cleaner Production* 2021; 318: 128452. https://doi.org/10.1016/j.jclepro.2021.128452.

[28] A. Mobasseri, M. Tostado-Véliz, A.A. Ghadimi, M. Reza-Miveh, F. Jurado. Multi-energy microgrid optimal operation with integrated power to gas technology considering uncertainties. *Journal of Cleaner Production* 2022; 333: 130174. https://doi.org/10.1016/j.jclepro.2021.130174.

[29] M. Gough et al. Operation of a Technical Virtual Power Plant Considering Diverse Distributed Energy Resources. *IEEE Transactions on Industry Applications*; Early access. https://doi.org/10.1109/TIA.2022.3143479.

[30] M. Tostado-Véliz, S. Kamel, H.M. Hasanien, R.A. Turky, F. Jurado. Uncertainty-aware day-ahead scheduling of microgrids considering response fatigue: An IGDT approach. *Applied Energy* 2022; 310: 118611. https://doi.org/10.1016/j.apenergy.2022.118611.

[31] A.R. Jordehi. Information gap decision theory for operation of combined cooling, heat and power microgrids with battery charging stations. *Sustainable Cities & Society* 2021; 74: 103164. https://doi.org/10.1016/j.scs.2021.103164.

[32] D.S. Falcão, A.M.F.R. Pinto. A review on PEM electrolyzer modelling: Guidelines for beginners. *Journal of Cleaner Production* 2020; 261: 121184. https://doi.org/10.1016/j.jclepro.2020.121184.

[33] D. Lim et al. Impact of voltage degradation in water electrolyzers on sustainability of synthetic natural gas production: Energy, economic, and environmental analysis. *Energy Conversion & Management* 2021; 245: 114516. https://doi.org/10.1016/j.enconman.2021.114516.

[34] X. Wu, H. Li, X. Wang, W. Zhao. Cooperative Operation for Wind Turbines and Hydrogen Fueling Stations With On-Site Hydrogen Production. *IEEE Transactions on Sustainable Energy* 2020; 11(4): 2775-89. https://doi.org/10.1109/TSTE.2020.2975609.

[35] M.S. Javadi et al. A two-stage joint operation and planning model for sizing and siting of electrical energy storage devices considering demand response programs. *International Journal of Electrical Power & Energy Systems* 2022; 138: 107912. https://doi.org/10.1016/j.ijepes.2021.107912.

[36] M. Inci, M. Büyük, M.H. Demir, G. Ilbey. A review and research on fuel cell electric vehicles: Topologies, power electronic converters, energy management methods, technical challenges, marketing and future aspects. *Renewable & Sustainable Energy Reviews* 2021; 137: 110648. https://doi.org/10.1016/j.rser.2020.110648.

[37] B. Faridpak, A. Alahyari, M. Farrokhifar, H. Momeni. Toward Small Scale Renewable Energy Hub-Based Hybrid Fuel Stations: Appraising Structure and Scheduling. *IEEE Transactions on Transportation Electrification* 2020; 6(1): 267-77. https://doi.org/10.1109/TTE.2020.2972382.

[38] J. Lv et al. Synergetic management of energy-water nexus system under uncertainty: An interval bi-level joint-probabilistic programming method. *Journal of Cleaner Production* 2021; 292: 125942. https://doi.org/10.1016/j.jclepro.2021.125942.

[39] B. Wang, C. Zhang, Z. Y. Dong. Interval Optimization Based Coordination of Demand Response and Battery Energy Storage System Considering SOC Management in a Microgrid. *IEEE Transactions on Sustainable Energy* 2020; 11(4): 2922-31. https://doi.org/10.1109/TSTE.2020.2982205.

[40] M. Tostado-Véliz, P. Arévalo, F. Jurado. An optimization framework for planning wayside and on-board hybrid storage systems for tramway applications. *Journal of Energy Storage* 2021; 43: 103207. https://doi.org/10.1016/j.est.2021.103207.

[41] S. Negarestani, M. Fotuhi-Firuzabad, M. Rastegar, A. Rajabi-Ghahnavieh. Optimal Sizing of Storage System in a Fast Charging Station for Plug-in Hybrid Electric Vehicles. *IEEE Transactions on Transportation Electrification* 2016; 2(4): 443-53. https://doi.org/10.1109/TTE.2016.2559165.

[42] X. Xu et al. Risk-based scheduling of an off-grid hybrid electricity/hydrogen/gas/ refueling station powered by renewable energy. *Journal of Cleaner Production* 2021; 315: 128155. https://doi.org/10.1016/j.jclepro.2021.128155.

[43] H. Rashidizadeh-Kermani, M. Vahedipour-Dahraie, A. Anvari-Moghaddam, J.M. Guerrero. A stochastic bi-level decision-making framework for a load-serving entity in day-ahead and balancing markets. *International Transactions on Electrical Energy Systems* 2019; 29(11): e12109. https://doi.org/10.1002/2050-7038.12109.

[44] G. Morrison, J. Stevens, F. Joseck. Relative economic competitiveness of light-duty battery electric and fuel cell electric vehicles. *Transportation Research Part C: Emerging Technologies* 2018; 87: 183-96. https://doi.org/10.1016/j.trc.2018.01.005.

[45] Z. Lin, J. Dong, C. Liu, D. Greene. Estimation of Energy Use by Plug-In Hybrid Electric Vehicles: Validating Gamma Distribution for Representing Random Daily Driving Distance. *Transportation Research Record: Journal of the Transportation Research Board* 2012; 2287: 37-43. https://doi.org/10.3141/2287-05.

[46] J. Kurtz, S. Sprik, G. Saur, S. Onorato. Fuel Cell Electric Vehicle Driving and Fueling Behavior. National Renewable Energy Laboratory, Rep. no. NREL/TP-5400-73010, 2019. Online, available at: https://www.nrel.gov/docs/fy19osti/73010.pdf, (accessed Feb. 22, 2022).

[47] S. Swaminathan, G.S. Pavlak, J. Freihaut. Sizing and dispatch of an islanded microgrid with energy flexible buildings. *Applied Energy* 2020; 276: 115355. https://doi.org/10.1016/j.apenergy.2020.115355.

[48] E.S. Pinto, L.M. Serra, A. Lázaro. Evaluation of methods to select representative days for the optimization of polygeneration systems. *Renewable Energy* 2020; 151: 488-502. https://doi.org/10.1016/j.renene.2019.11.048.

[49] M. Daneshvar, B. Mohammadi-Ivatloo, K. Zare, S. Asadi, A. Anvari-Moghaddam. A Novel Operational Model for Interconnected Microgrids Participation in Transactive Energy Market: A Hybrid IGDT/Stochastic Approach. *IEEE Transactions on Industrial Informatics* 2021; 17(6): 4025-35. https://doi.org/10.1109/TII.2020.3012446.

[50] C. Lork et al. An uncertainty-aware deep reinforcement learning framework for residential air conditioning energy management. *Applied Energy* 2020; 276: 115426. https://doi.org/10.1016/j.apenergy.2020.115426.

[51] Gurobi Optimization L.L.C. Gurobi Optimizer Reference Manual, 2021. Online, available at: https://www.gurobi.com, (accessed Feb. 23, 2022).

[52] K.B. de Oliveira, E.F. dos Santos, A.F. Neto, V.H. de Mello Santos, O.J. de Oliveira. Guidelines for efficient and sustainable energy management in hospital buildings. *Journal of Cleaner Production* 2021; 329: 129644. https://doi.org/10.1016/j.jclepro.2021.129644.

[53] M. Jooshaki, H. Farzin, A. Abbaspour, M. Fotuhi-Firuzabad, M. Lehtonen. A Model for Stochastic Planning of Distribution Network and Autonomous DG Units. *IEEE Transactions on Industrial Informatics* 2020; 16(6): 3685-96. https://doi.org/10.1109/TII.2019.2936280.

[54] European Commission. Photovoltaic Geographical Information System. Online, available at: https://re.jrc.ec.europa.eu/pvg_tools/en/tools.html, (accessed Feb. 23, 2022).

[55] Engie. Historical data reports. Online, available at: https://www.engieresources.com/historical-data#reports_anchor, (accessed Feb. 23, 2022).

[56] M.S. Javadi, M. Lotfi, A.E. Nezhad, A. Anvari-Moghaddam, J.M. Guerrero, J.P.S. Catalão. Optimal Operation of Energy Hubs Considering Uncertainties and Different Time Resolutions. *IEEE Transactions on Industry Applications* 2020; 56(5): 5543-52. https://doi.org/10.1109/TIA.2020.3000707.

[57] California Fuel Cell Parnertship. Cost to refill. Online, available at: https://cafcp.org/content/cost-refill, (accessed Feb. 23, 2022).

[58] G. Parks, R. Boyd, J. Cornish, R. Remick. Hydrogen Station Compression, Storage, and Dispensing Technical Status and Costs. National Renewable Energy Laboratory, Rep. no. NREL/BK-6A10-58564, 2014. Online, available at: https://www.nrel.gov/docs/fy14osti/58564.pdf, (accessed Feb. 23, 2022).

[59] Hydrogen Council. Path to Hydrogen competitiveness. A cost perspective. 2020. Online, available at: https://hydrogencouncil.com/wp-content/uploads/2020/01/Path-to-Hydrogen-Competitiveness_Full-Study-1.pdf, (accessed Feb. 23, 2022).

[60] F. Canavero. *Uncertainty Modeling for Engineering Applications*. Cham, Switzerland: Springer Nature; 2019.